Electronic Supplementary Material (ESI) for Journal of Materials Chemistry C.
This journal is © The Royal Society of Chemistry 2020

Bright and efficient red emitting electroluminescent devices containing a ternary europium complex with greater than 6% external quantum efficiency

Rashid Ilmi,*[a] Muhammad S. Khan*,[a] Weidong Sun[b], José D. L. Dutra[c], Willyan F. Oliveira[c], Liang Zhou*,[b] Wai-Yeung Wong*[d], Paul R. Raithby*[e]

[a]Department of Chemistry, Sultan Qaboos University, P. O. Box 36, Al Khod 123,

[b]State Key Laboratory of Rare Earth Resource Utilization, Changchun Institute of Applied Chemistry, Chinese Academy of Sciences, Renmin Street 5625, Changchun 130022, People's Republic of China.

[c]Pople Computational Chemistry Laboratory, Department of Chemistry, UFS, 49100-000 São Cristóvão, Sergipe, Brazil

[d]Department of Applied Biology and Chemical Technology, The Hong Kong Polytechnic University, Hung Hom, Kowloon, Hong Kong.

[e]Department of Chemistry, University of Bath, Claverton Down, Bath BA2 7AY, UK

Addresses and ORCID ID of corresponding authors:

Rashid Ilmi **:** rashidilmi@gmail.com; 0000-0002-5165-5977

Muhammad S. Khan **:** msk@squ.edu.om; 0000-0001-5606-6832

Liang Zhou **:** zhoul@ciac.ac.cn; 0000-0002-2751-5974

Paul R. Raithby : p.r.raithby@bath.ac.uk; 0000-0002-2944-0662

Wai-Yeung Wong **:** wai-yeung.wong@polyu.edu.hk; 0000-0002-9949-7525

Supporting Information

Contents

1. Synthesis of Binary hydrated complexes

1.1. [Eu(btfa)$_3$(H$_2$O)$_2$] and [Eu(nta)$_3$(H$_2$O)$_2$]

Binary hydrated [Eu(btfa)$_3$(H$_2$O)$_2$] and [Eu(nta)$_3$(H$_2$O)$_2$] complexes (**Chart S1**) were synthesized by the conventional method.[1] Briefly, EuCl$_3$.6H$_2$O (Eu- 2.39 g, 6.57 mmol) aqueous solution was added dropwise through a dropping funnel to a solution of sodium salt of β-diketone (2.0 g, 19.97 mmol). The precipitate formed was filtered, washed with a copious amount of deionized water and dried in vacuum over P$_4$O$_{10}$ and re-crystallized from DCM.

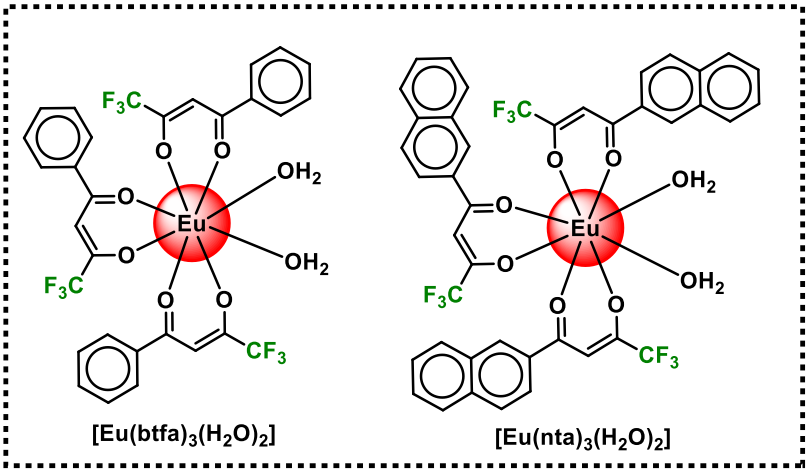

Chart S1: Chemical structures of binary hydrated [Eu(btfa)$_3$(H$_2$O)$_2$] and [Eu(nta)$_3$(H$_2$O)$_2$] complexes

2. Theoretical Judd–Ofelt (J-O) intensity parameters (Ω$_\lambda$) (λ = 2, 4 and 6)

The theoretical intensity parameters derived from the Judd-Ofelt theory[2] were calculated by the following expression[3]:

$$\Omega_\lambda^{calc} = (2\lambda+1)\sum_{t}^{\lambda-1,\lambda+1(odd)}\sum_{p=-t}^{t(all)}\frac{\left|B_{\lambda tp}\right|^2}{(2t+1)} \qquad \text{Eq. S1}$$

$$B_{\lambda tp} = \frac{2}{\Delta E}\left\langle r^{t+1}\right\rangle\theta(t,\lambda)\gamma_p^t - \left[\frac{(\lambda+1)(2\lambda+3)}{2\lambda+1}\right]^{1/2}\left\langle r^{\lambda}\right\rangle(1-\sigma_\lambda)\left\langle f\left\|C^{(\lambda)}\right\|f\right\rangle\Gamma^t_p\delta_{t,\lambda+1} \qquad \text{Eq. S2}$$

$$\gamma_p^t = \left(\frac{4\pi}{2t+1}\right)^{1/2} e^2 \sum_j \rho_j \left(2\beta_j\right)^{t+1} \frac{g_j}{R_j^{t+1}} Y_p^{t*}\left(\theta_j, \phi_j\right) \qquad \text{Eq. S3}$$

$$\Gamma_p^t = \left(\frac{4\pi}{2t+1}\right)^{1/2} \sum_j \frac{\alpha_j}{R_j^{t+1}} Y_p^{t*}\left(\theta_j, \phi_j\right) \qquad \text{Eq. S4}$$

The distance from atom *j* coordinated directly to the lanthanide ion (R_j) together with the corresponding angular coordinates (θ_j and ϕ_j) show the dependency of the theoretical intensity parameters on the complex structure. Eq. S2 contains the contribution from the forced electric dipole and dynamic coupling mechanisms. The theoretical Ω_λ have been calculated by adjusting the charge factors (g_j) and polarizabilities (α_j), Eq. S3 and S4, respectively, in order to reproduce the experimental values of Ω_2 and Ω_4. The complete procedure used to calculate Ω_λ is widely discussed in reference.[4]

The *QDC* model[4] implemented into LUMPAC[5] postulates that the g_j are obtained from the product between adjustable parameters (*Q*) and each ZDO (*Zero Differential Overlap*) electronic density (q_j) of each atom *j* coordinated directly to the lanthanide ion. Similarly, the *QDC* model postulates that the α_j are calculated using two adjustable parameters (*D* and *C*)

$$g_j = Q.q_j \qquad \text{Eq. S5}$$

$$\alpha_j = SE_j \cdot D + C \qquad \text{Eq. S6}$$

The ZDO electronic density and the electrophilic superdelocalizability (*SE*) for any atom μ of the complex are calculated by

$$q_\mu = 2\sum_{i'}^{occ.} \sum_p^{N_\mu} \left|c_{pi'}^\mu\right|^2 \qquad \text{Eq. S7}$$

$$SE_\mu = 2\sum_{i'}^{occ.} \sum_p \sum_q \frac{c_{pi'}^\mu c_{qi'}^\mu}{\varepsilon_{i'}} \qquad \text{Eq. S8}$$

where *i'* runs through all the occupied molecular orbitals of the complex, *p* runs through all atomic orbitals, $c_{pi'}^\mu$ is the corresponding linear coefficient, and ε_i is the energy of the occupied molecular orbital *i*.

The theoretical radiative decay rate for europium is given by

$$A_{rad} = \frac{32e^2\pi^3\chi}{3\hbar\left(2J+1\right)} \sum_{\lambda=2,4,6} \nu[^5D_0 \rightarrow {}^7F_{J=\lambda}]^3\Omega_\lambda \left|\left\langle {}^5D_0 \left\| U^{(\lambda)} \right\| {}^7F_{J=\lambda} \right\rangle\right|^2 + \frac{32\pi^3 n^3 \nu[^5D_0 \rightarrow {}^7F_1]^3}{3\hbar} S_{md} \qquad \text{Eq. S9}$$

where *e* is the elementary charge; 2*J*+1 is the degeneracy of the initial state, in this case $^5D_0$, and therefore *J*=0. χ is the Lorentz local-field correction term given by $\chi = n(n^2+2)^2/9$, in this work value of refractive index *n* equal to 1.424 was considered. $\nu[^5D_0 \rightarrow {}^7F_J]$ are the energies of the barycenters of the respective transitions. The magnetic dipole strength of the $^5D_0 \rightarrow {}^7F_1$ transition is theoretically evaluated as being S_{md} = 9,6 × 10^{-42} esu^2cm^2 [6].

3. Theoretical Quantum Yield

The PLQY (*q*) is defined as the ratio of the number of emitted photons by the lanthanide ion to the number of absorbed photons by the ligand.

$$q = \frac{A_{rad}\eta_{^5D_0}}{\varphi\eta_{S_0}} \qquad \text{Eq. S10}$$

where the terms η_{S_0} and $\eta_{^5D_0}$ correspond to the energetic population of the S_0 and $^5D_0$ states, respectively. φ is the absorption rate from the fundamental singlet to the excited singlet of the ligand. The normalized population of a given level *j* considered in the energy transfer modeling, η_j, are obtained from an equations system in the steady-state approximation.

$$\frac{d\eta_j}{dt} = -\sum_{i\neq j} W_{ji}\eta_j + \sum_{i\neq j} W_{ij}\eta_i \qquad \text{Eq. S11}$$

11where W_{ij} is the transfer rate from level *i* to level *j*, with the transition rates from and to the same state are zero. In the steady-state approximation $\frac{d\eta_j}{dt} = 0$, allowing that the set of algebraic equations derived from Eq. S11 can be solved analytically. The emission quantum yield for the complexes were calculated with LUMPAC 1.4.0.[5]

4. Full EL Device structures

4.1 Single EML Device based on Eu-1

Device 1: ITO/HAT-CN (6 nm)/HAT-CN (0.2 wt%): TAPC (50 nm)/**Eu-1** (3 wt%): 26DCzPPy (10 nm)/Tm3PyP26PyB (60 nm)/LiF (1 nm)/Al (100 nm)

Device 2: ITO/HAT-CN (6 nm)/HAT-CN (0.2 wt%): TAPC (50 nm)/**Eu-1** (4 wt%): 26DCzPPy (10 nm)/Tm3PyP26PyB (60 nm)/LiF (1 nm)/Al (100 nm)

Device 3: ITO/HAT-CN (6 nm)/HAT-CN (0.2 wt%): TAPC (50 nm)/**Eu-1** (5 wt%): 26DCzPPy (10 nm)/Tm3PyP26PyB (60 nm)/LiF (1 nm)/Al (100 nm)

4.2 Double EML Device based on Eu-1

Device 4: ITO/HAT-CN (6 nm)/HAT-CN (0.2 wt%): TAPC (50 nm)/**Eu-1** (3 wt%): TcTa (10 nm)/**Eu-1** (3 wt%): 26DCzPPy (10 nm)/Tm3PyP26PyB (60 nm)/LiF (1 nm)/Al (100 nm)

Device 5: ITO/HAT-CN (6 nm)/HAT-CN (0.2 wt%): TAPC (50 nm)/**Eu-1** (4 wt%): TcTa (10 nm)/**Eu-1** (4 wt%): 26DCzPPy (10 nm)/Tm3PyP26PyB (60 nm)/LiF (1 nm)/Al (100 nm)

Device 6: ITO/HAT-CN (6 nm)/HAT-CN (0.2 wt%): TAPC (50 nm)/**Eu-1** (5 wt%): TcTa (10 nm)/**Eu-1** (5 wt%): 26DCzPPy (10 nm)/Tm3PyP26PyB (60 nm)/LiF (1 nm)/Al (100 nm)

4.3 Single EML Device based on Eu-2

Device 1: ITO/HAT-CN (6 nm)/HAT-CN (0.2 wt%): TAPC (50 nm)/**Eu-2** (3 wt%): 26DCzPPy (10 nm)/Tm3PyP26PyB (60 nm)/LiF (1 nm)/Al (100 nm)

Device 2: ITO/HAT-CN (6 nm)/HAT-CN (0.2 wt%): TAPC (50 nm)/**Eu-2** (4 wt%): 26DCzPPy (10 nm)/Tm3PyP26PyB (60 nm)/LiF (1 nm)/Al (100 nm)

Device 3: ITO/HAT-CN (6 nm)/HAT-CN (0.2 wt%): TAPC (50 nm)/**Eu-2** (5 wt%): 26DCzPPy (10 nm)/Tm3PyP26PyB (60 nm)/LiF (1 nm)/Al (100 nm)

4.4 Double EML Device based on Eu-2

Device 4: ITO/HAT-CN (6 nm)/HAT-CN (0.2 wt%): TAPC (50 nm)/**Eu-2** (3 wt%): TcTa (10 nm)/**Eu-2** (3 wt%): 26DCzPPy (10 nm)/Tm3PyP26PyB (60 nm)/LiF (1 nm)/Al (100 nm)

Device 5: ITO/HAT-CN (6 nm)/HAT-CN (0.2 wt%): TAPC (50 nm)/**Eu-2** (4 wt%): TcTa (10 nm)/**Eu-2** (4 wt%): 26DCzPPy (10 nm)/Tm3PyP26PyB (60 nm)/LiF (1 nm)/Al (100 nm)

Device 6: ITO/HAT-CN (6 nm)/HAT-CN (0.2 wt%): TAPC (50 nm)/**Eu-2** (5 wt%): TcTa (10 nm)/**Eu-2** (5 wt%): 26DCzPPy (10 nm)/Tm3PyP26PyB (60 nm)/LiF (1 nm)/Al (100 nm)

Table S1. Corrected emission intensity relative to $^5D_0 \rightarrow {}^7F_1$ transition, Barycenter, %contribution of each transition of **Eu-1** and **Eu-2** in DCM solution at RT

	Corrected emission Intensity relative to $^5D_0 \rightarrow {}^7F_1$ transition					
	$\int 0-0$	$\int 0-1$	$\int 0-2$	$\int 0-3$	$\int 0-4$	$\int total$
Eu-1						
Corrected intensity[a]	0.24	1.00	18.89	0.63	2.06	22.82
Barycenter (cm^{-1})	17253.59	16883.65	16214.77	15310.25	14338.68	
%contribution	1.05%	-	82.77%	2.76%	9.02%	
Eu-2						
Corrected intensity[a]	0.23	1.00	20.42	0.61	2.21	24.47
Barycenter (cm^{-1})	17261.37	16881.43	16218.07	15322.58	(14337.79)	
%contribution	[0.93%]	-	[83.44%]	[2.49%]	[9.03%]	

[a]relative to the MD $^5D_0 \rightarrow {}^7F_1$ transition

Table S2. Sparkle/RM1 model ZDO electronic densities (*q*) and electrophilic superdelocalizabilities (*SE*), by considering the B3LYP/SVP/MWB52 geometry, for each atom directly coordinated to Eu^{3+}, in complexes **Eu-1** and **Eu-2**, together with corresponding charge factors (*g*) and polarizabilities (α) from the fitting. Calculated electric dipole intensity parameters (Ω_λ^{FED}) for both complexes

Ligand Atom	**Eu-1**				**Ligand Atom**	**Eu-2**			
	Q = 0.0169 au^{-1} *D* = 40.58 $au^{-1}\cdot Å^3$ *C* = 19.32 $Å^3$ *D/C* = 2.10 au^{-1}					*Q* = 0.0319 au^{-1} *D* = 42.32 $au^{-1}\cdot Å^3$ *C* = 20.41 $Å^3$ *D/C* = 2.07 au^{-1}			
	q **(au)**	***SE*** **(au)**	***g***	**α (Å³)**		***q*** **(au)**	***SE*** **(au)**	***g***	**α (Å³)**
O(DPEPO)	6.8450	-0.4289	0.1160	1.9161	O(DPEPO)	6.8477	-0.4163	0.2187	2.7914
O(DPEPO)	6.8338	-0.4360	0.1158	1.6286	O(DPEPO)	6.8325	-0.4376	0.2182	1.8937
O(btfa1)	6.3177	-0.4089	0.1070	2.7268	O(nta1)	6.3191	-0.4194	0.2018	2.6610
O(btfa)	6.3435	-0.4347	0.1075	1.6815	O(nta1)	6.3427	-0.4484	0.2026	1.4357
O(btfa2)	6.3395	-0.4184	0.1074	2.3415	O(nta2)	6.3447	-0.4309	0.2026	2.1759
O(btfa2)	6.3447	-0.4614	0.1075	0.5954	O(nta2)	6.3242	-0.4677	0.2020	0.6177
O(btfa3)	6.3367	-0.2841	0.1074	7.7923	O(nta3)	6.3396	-0.3013	0.2025	7.6614
O(btfa3)	6.3313	-0.2341	0.1073	9.8193	O(nta3)	6.3401	-0.2370	0.2025	10.3838
	$\Omega_2^{FED} = 0.0001\times10^{-20}$ cm^2 $\Omega_4^{FED} = 0.0022\times10^{-20}$ cm^2 $\Omega_6^{FED} = 0.0049\times10^{-20}$ cm^2					$\Omega_2^{FED} = 0.0005\times10^{-20}$ cm^2 $\Omega_4^{FED} = 0.0079\times10^{-20}$ cm^2 $\Omega_6^{FED} = 0.0167\times10^{-20}$ cm^2			

Table S3. Singlet and triplet excited states energy and corresponding distance from the Eu(III) nucleus to the electronic barycenter of the ligand donor state (R_L) for the different RM1 geometries considered for the **Eu-1** and **Eu-2** complexes

Complex	$R_{L,sing.}$ (Å)	$E_{sing.}$ (cm^{-1})	$R_{L,trip.}$ (Å)	$E_{trip.}$ (cm^{-1})
INDO/S-CIS // RM1				
Eu-1				
Eu-1-1	3.97	36058.9	4.90	20720.2
Eu-1-2	3.81	35713.3	4.69	20721.7
Eu-1-3	4.30	35983.9	4.89	20896.7
Eu-1-4	4.28	36604.6	3.98	21038.4
Eu-1-5	4.51	36227.7	4.69	20969.0
Eu-1-6	4.25	36402.8	4.49	20935.9
Eu-1-7	4.08	35751.6	4.25	20865.5
Eu-1-8	4.35	36122.6	4.60	20890.1
Eu-2				
Eu-2-1	5.25	34962.9	5.49	20959.6
Eu-2-2	4.87	35752.2	5.95	22009.4
Eu-2-3	4.91	35883.7	5.52	21166.7
Eu-2-4	5.57	36389.0	5.49	21058.1
Eu-2-5	5.34	36956.9	5.54	21203.7
Eu-2-6	5.45	36321.3	5.69	21120.7
Eu-2-7	5.16	36546.1	5.47	21180.7
Eu-2-8	5.27	36884.1	5.50	21128.2

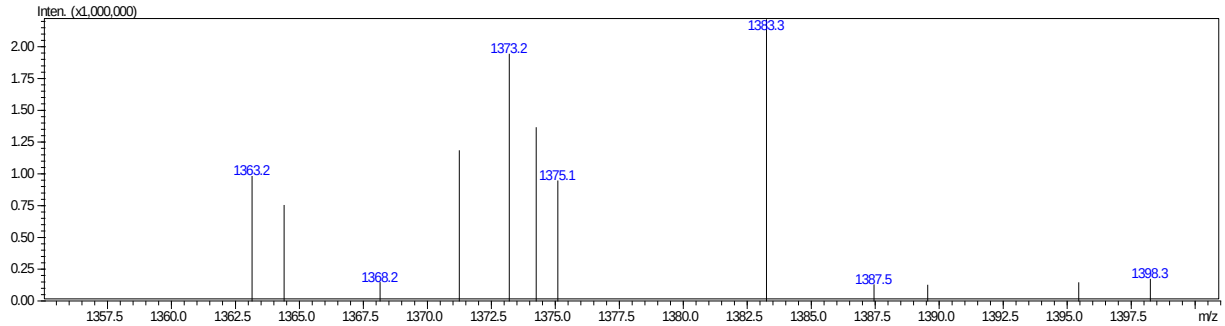

Fig. S1. Positive mode ESI-MS spectrum of **Eu-1** complex in acetone solution**.**

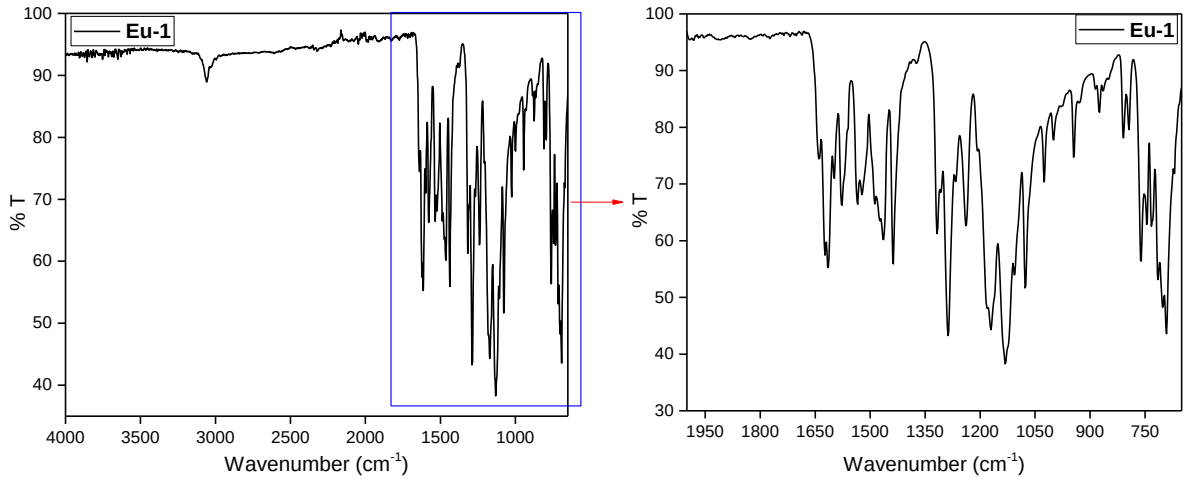

Fig. S2. FTI-R spectrum of solid **Eu-1** complex with its expansion from 2000 – 650 cm^{-1}.

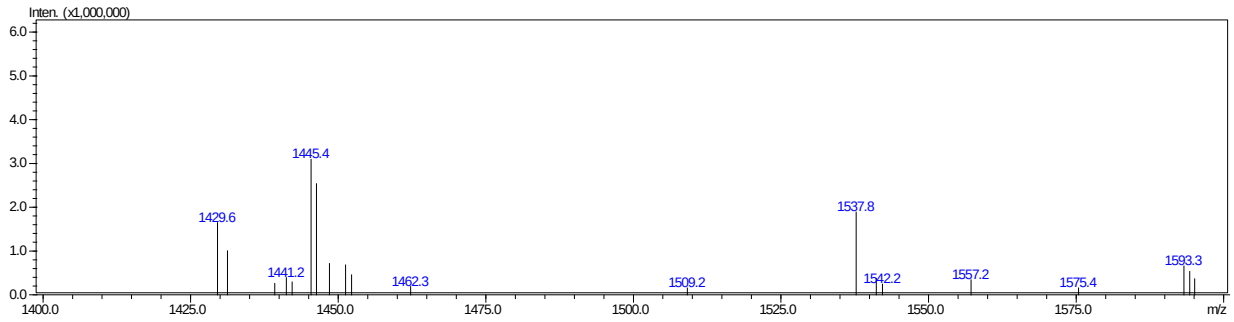

Fig. S3. Positive mode ESI-MS spectrum of **Eu-2** complex in acetone solution**.**

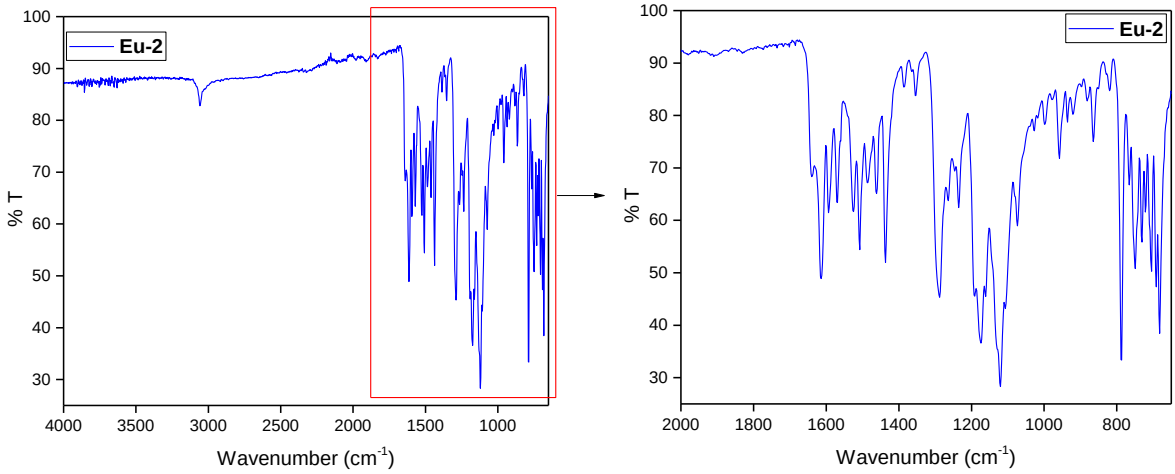

Fig. S4. FTI-R spectra of solid **Eu-2** complex with its expansion from 2000 – 650 cm^{-1}.

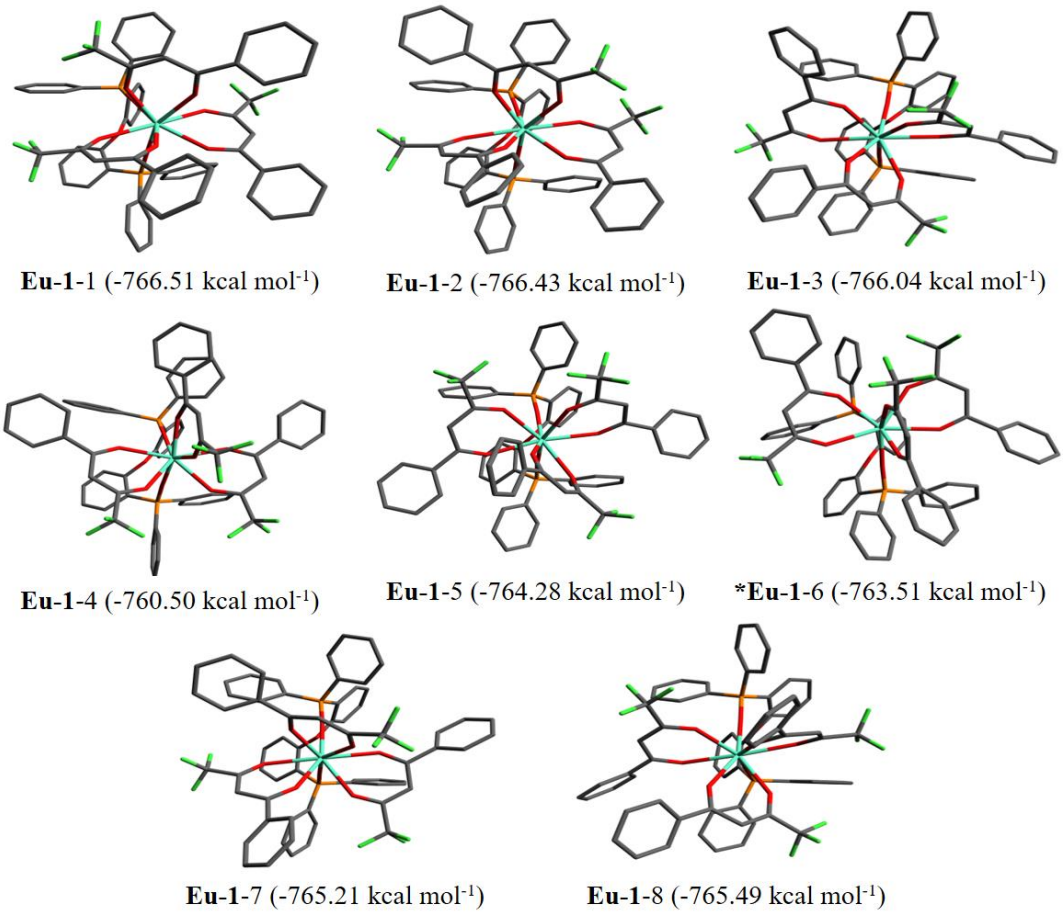

Fig. S5. Geometries optimized at the RM1 level of theory for different structural possibilities considered for **Eu-1**. The values in the parentheses are the heat of formation for each structure calculated with RM1. *Conformation of the starting structure (CSD CODE 1942486).

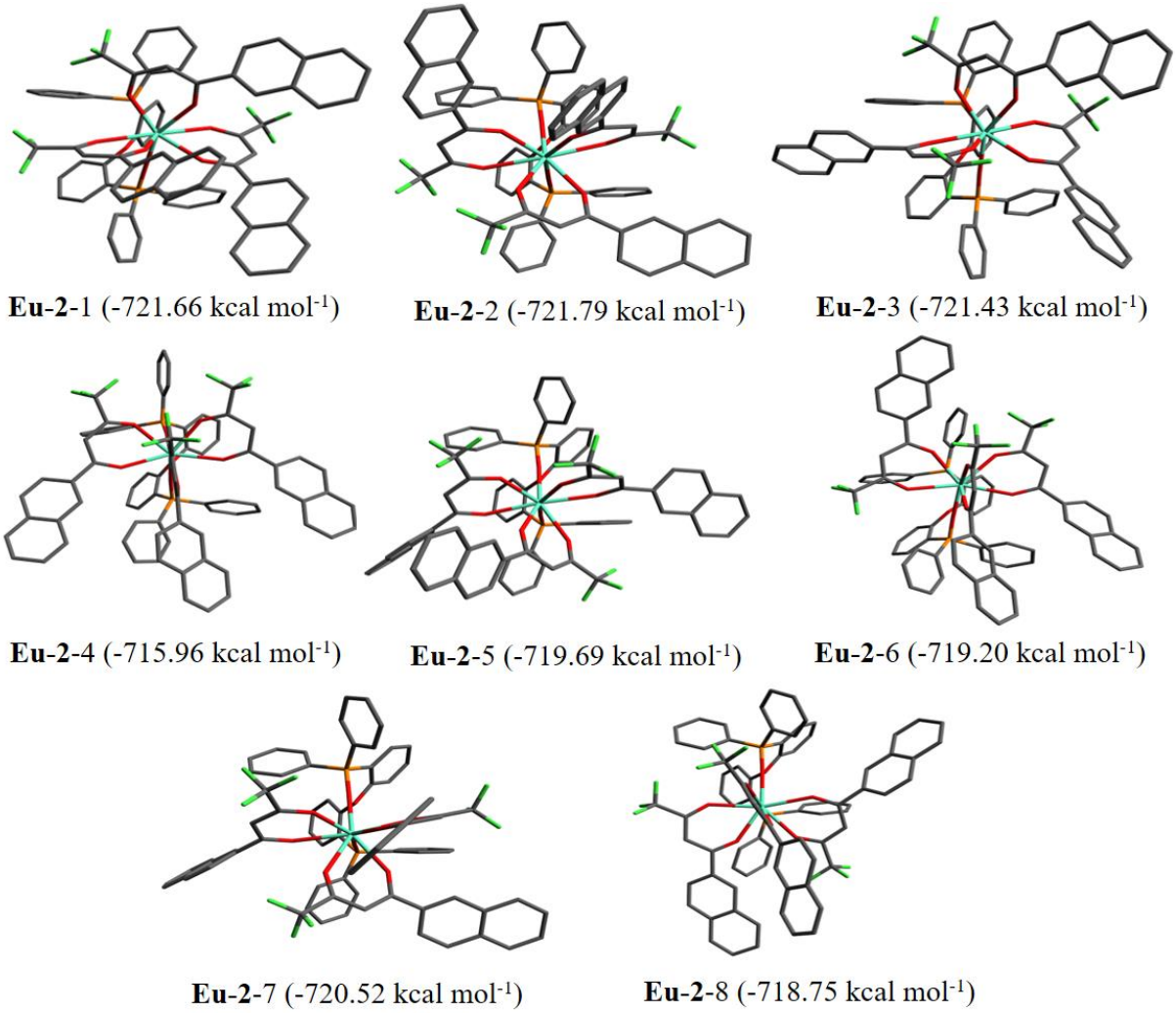

Fig. S6. Geometries optimized at the RM1 level of theory for different structural possibilities considered for **Eu-2** complex. The values in the parentheses are the heat of formation for each structure calculated with RM1.

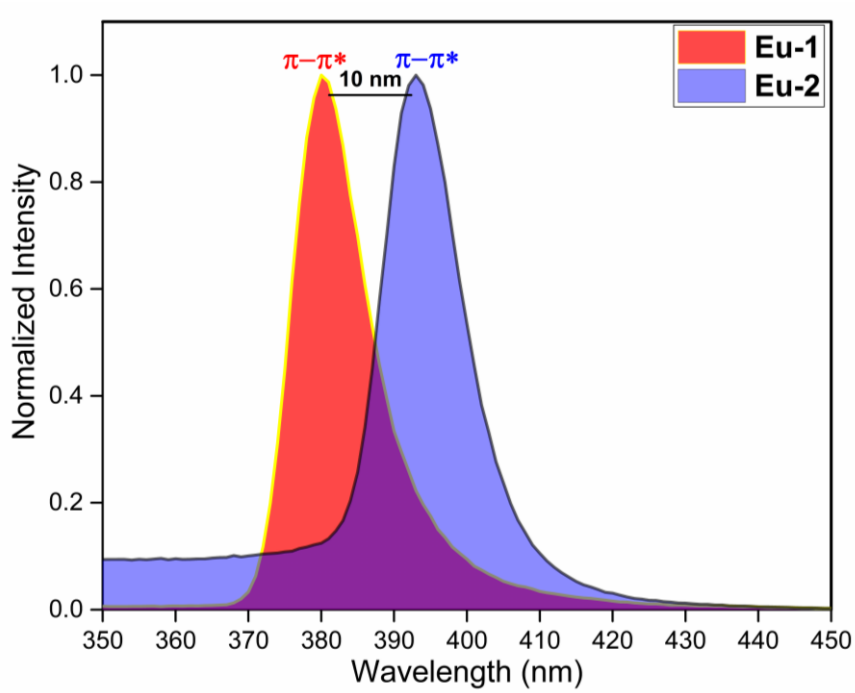

Fig. S7. Excitation spectra of the **Eu-1** and **Eu-2** complexes in DCM solution at RT.

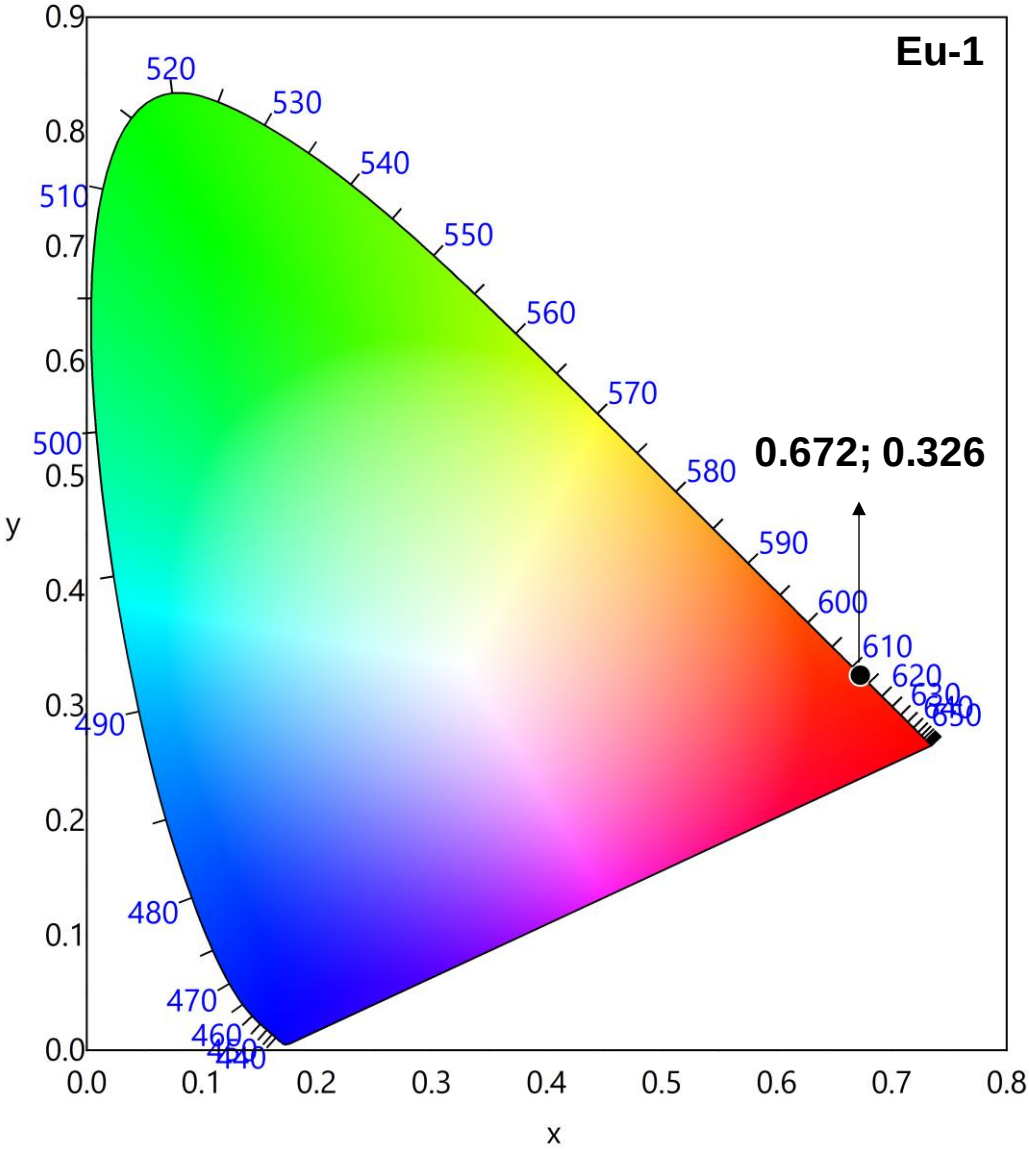

Fig. S8. International Commission on Illumination (CIE) 1931 chromaticity diagram of **Eu-1** showing the observed color in DCM solution at RT.

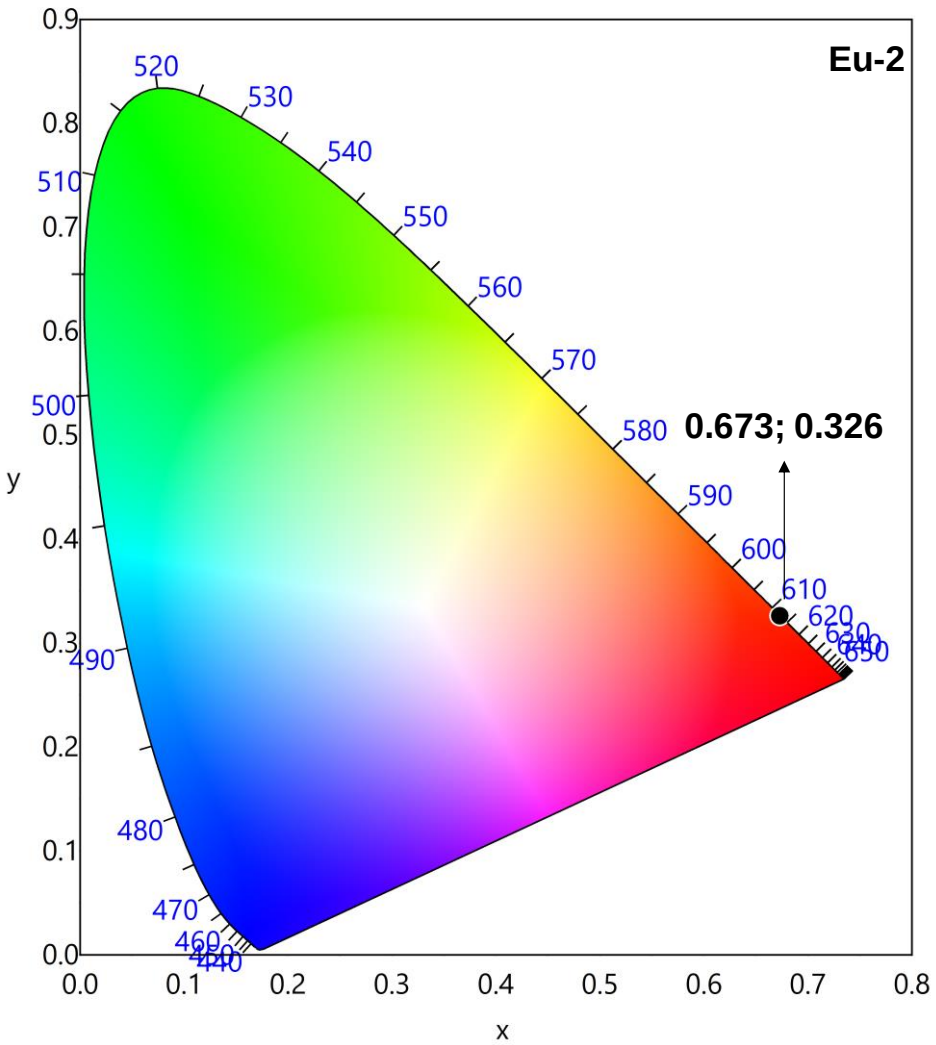

Fig. S9. 1931 CIE chromaticity diagram of **Eu-2** showing the observed color in DCM solution at RT.

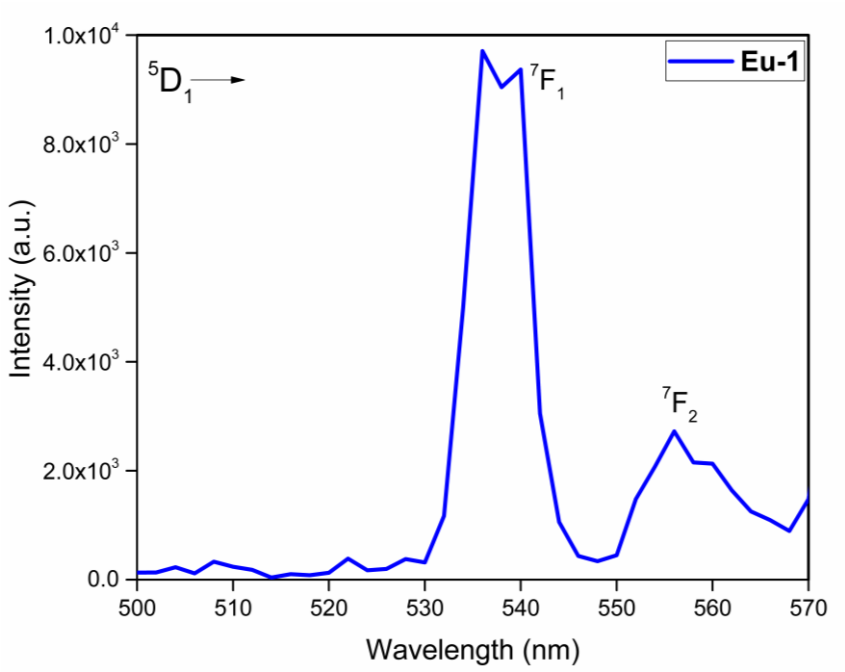

Fig. S10. Magnification of the region between 500 – 570 nm displaying $^5D_1 \rightarrow {}^7F_{1-2}$ transitions at RT for **Eu-1** complex.

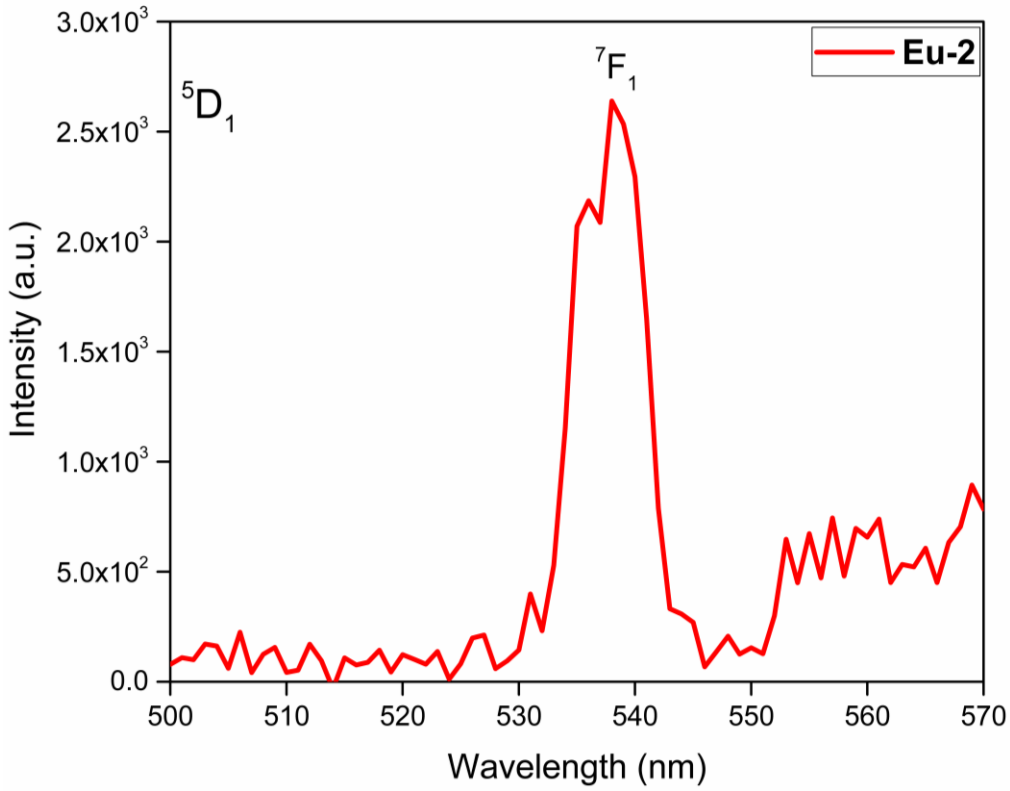

Fig. S11. Magnification of the region between 500 – 570 nm displaying $^5D_1 \rightarrow {}^7F_1$ transitions at RT for **Eu-2** complex.

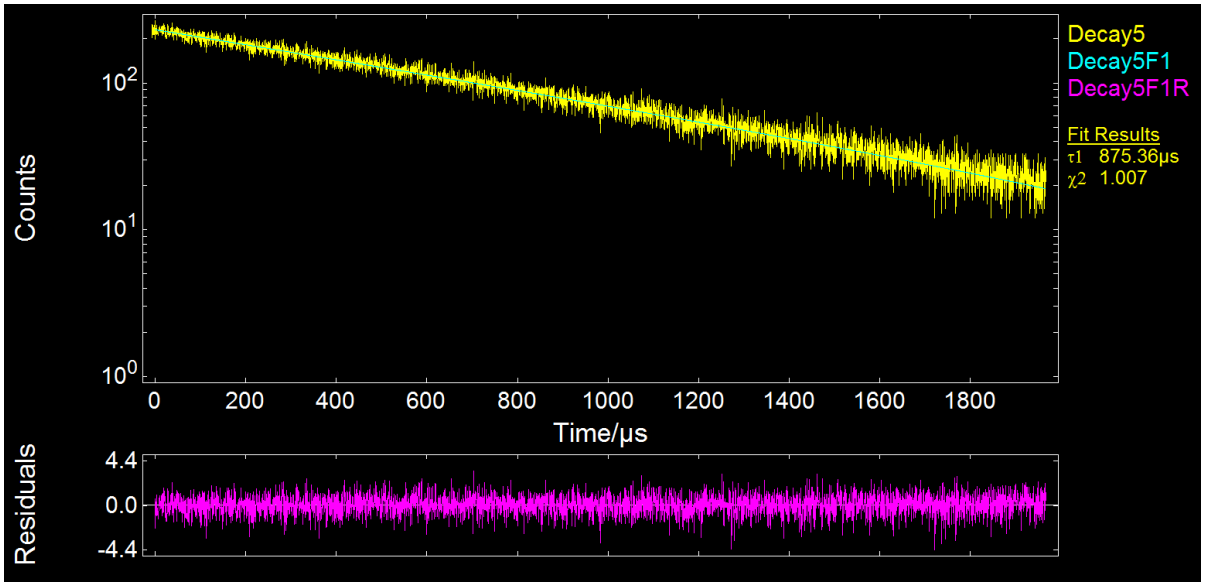

Fig. S12. Decay curve of **Eu-1** with fitted curve and observed luminescence lifetime in DCM at RT.

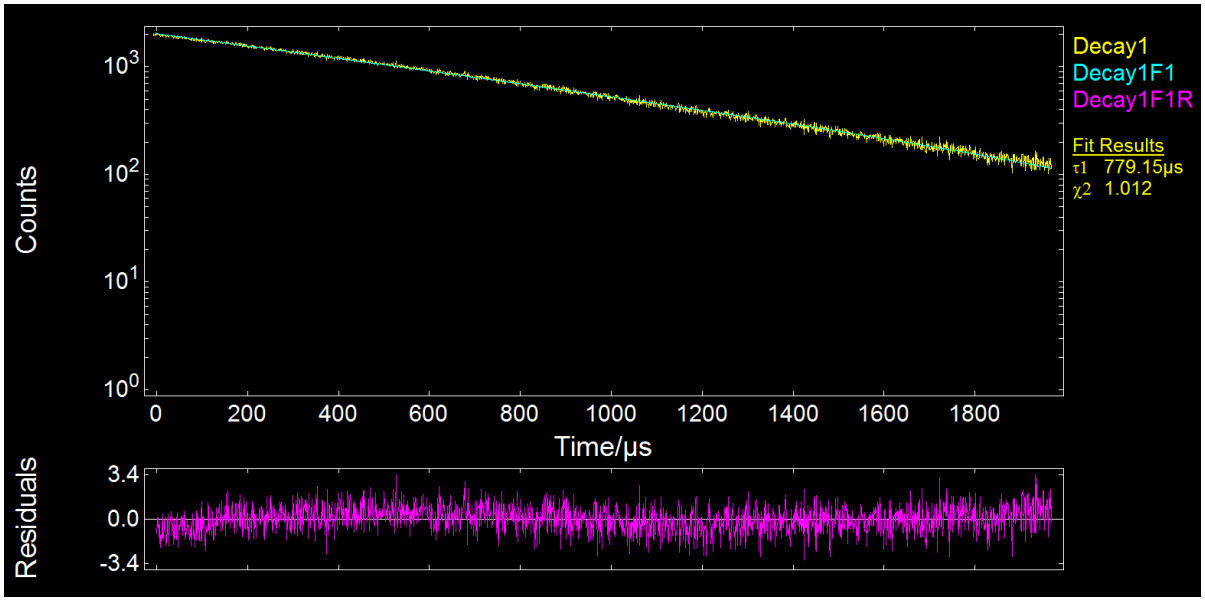

Fig. S13. Decay curve of **Eu-2** with fitted curve and observed luminescence lifetime in DCM at RT.

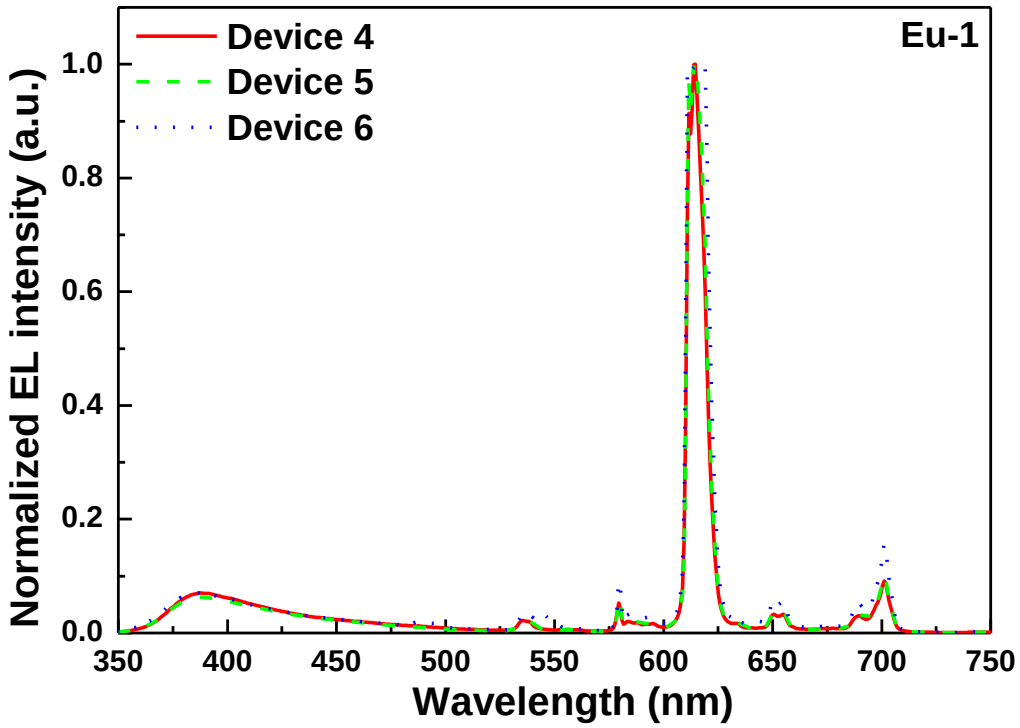

Fig. S14. Normalized EL spectra of the double-EML devices **4**, **5** and **6** of **Eu-1** operating at 10 mA/cm^2.

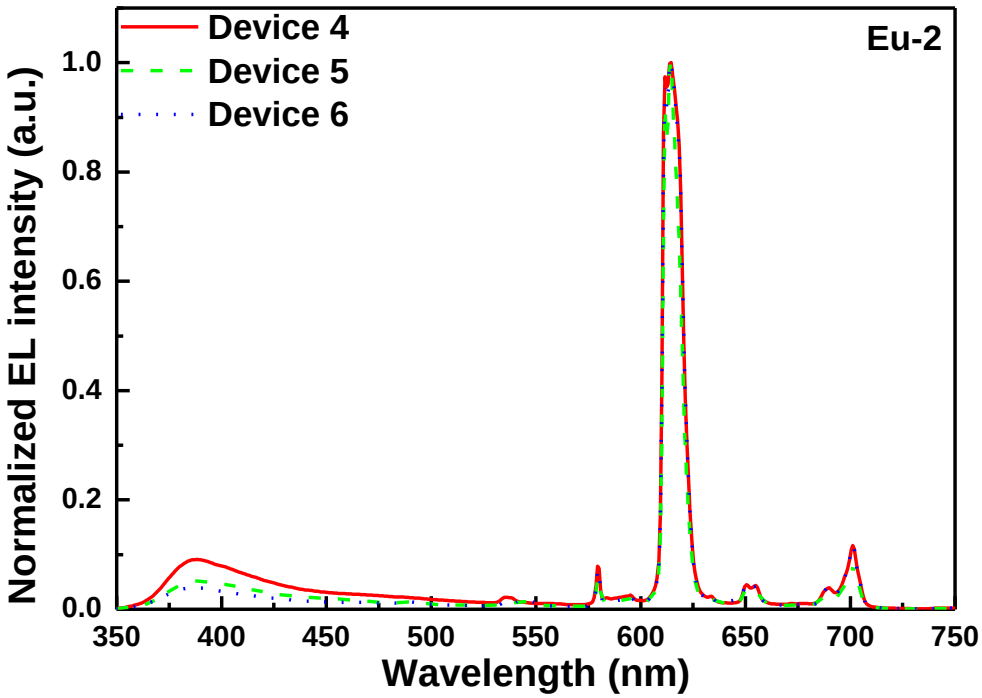

Fig. S15. **Normalized EL spectra of the double-EML devices** 4, 5 **and** 6 **of** Eu-2 **operating at 10 mA/cm^2.**

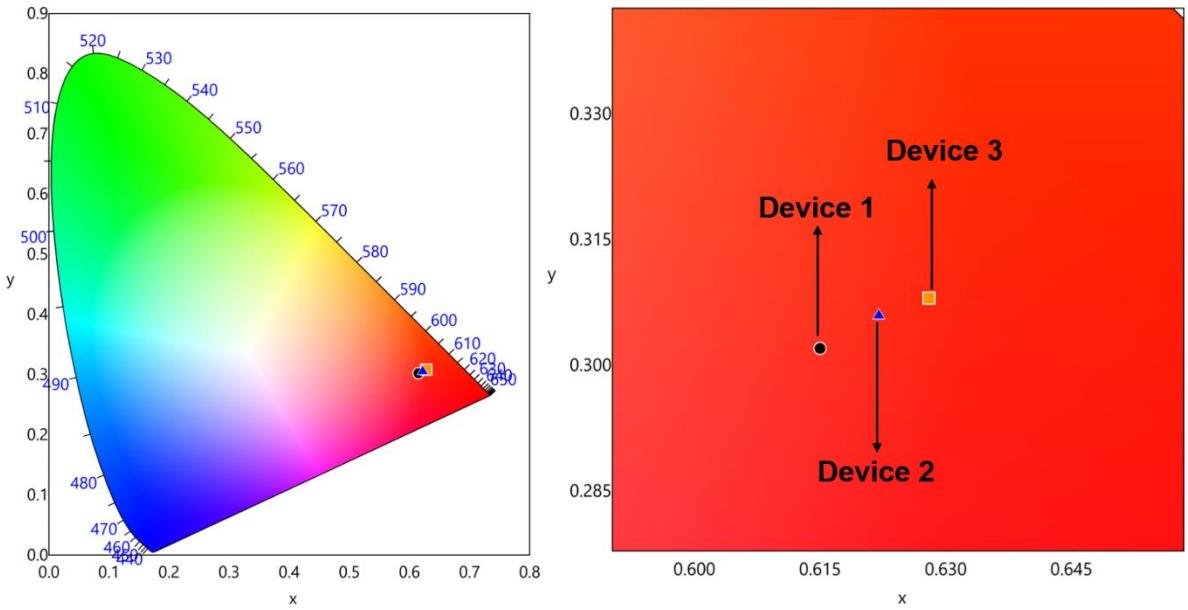

Fig. S16. CIE 1931 chromaticity diagrams of single EML devices **1**, **2** and **3** of **Eu-2** with magnified view operating at 10 mA/cm^2.

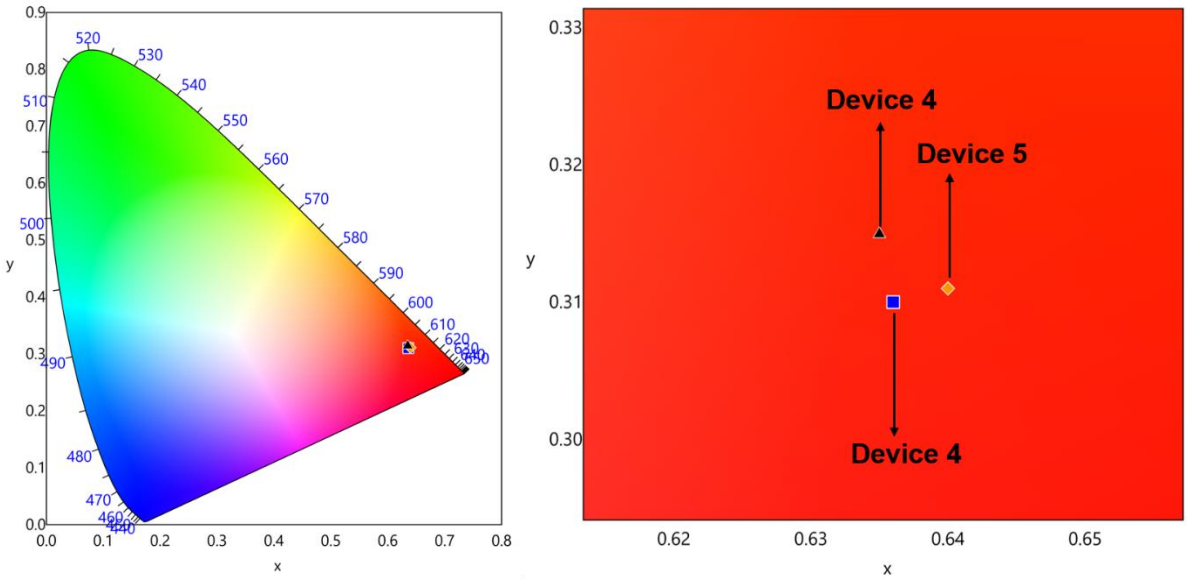

Fig. S17. CIE 1931 chromaticity diagrams of single EML devices **4**, **5** and **6** of **Eu-1** with magnified view operating at 10 mA/cm^2.

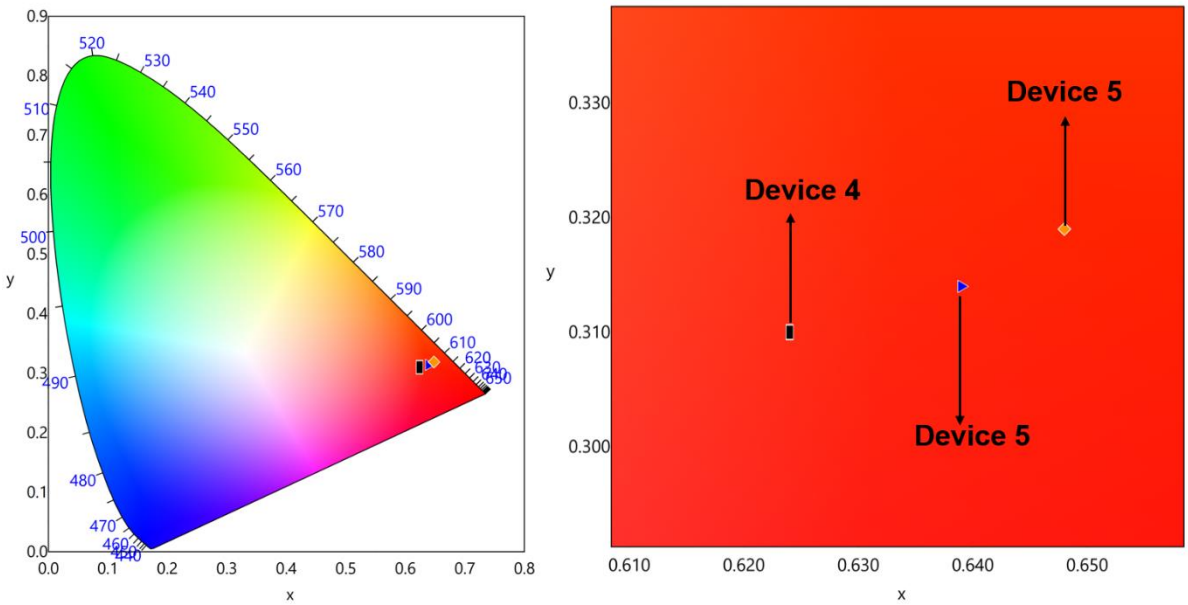

Fig. S18. CIE 1931 chromaticity diagrams of single EML devices **4**, **5** and **6** of **Eu-2** with magnified view operating at 10 mA/cm^2.

References

1. L. R. Melby, N. J. Rose, E. Abramson and J. C. Caris, *J. Am. Chem. Soc.*, 1964, **86**, 5117-5125.
2. (a) B. R. Judd, *Phys. Rev.* , 1962, **127**, 750-761; (b) G. S. Ofelt, *J. Chem. Phys.*, 1962, **37**, 511-520.
3. G. F. de Sa, O. L. Malta, C. D. Donega, A. M. Simas, R. L. Longo, P. A. Santa-Cruz and E. F. da Silva, *Coordin Chem Rev*, 2000, **196**, 165-195.
4. J. D. L. Dutra, N. B. D. Lima, R. O. Freire and A. M. Simas, *Sci. Rep.*, 2015, **5**, 13695.
5. J. D. Dutra, T. D. Bispo and R. O. Freire, *J. Comput. Chem.*, 2014, **35**, 772-775.
6. M. J. Weber, T. E. Varitimo and B. H. Matsinge, *Phys Rev B*, 1973, **8**, 47-53.